Influence of heterogeneity patterns on active and passive spreading and reaction during in situ groundwater remediation

R.M. Neupauer, Ph.D., P.E., F.ASCE,[1] F.C. Rankin, EIT[2]

[1] Department of Civil, Environmental, and Architectural Engineering, University of Colorado Boulder, UCB 428, ECOT 441, Boulder, CO 80309-0248; email: neupauer@colorado.edu
[2] Department of Civil, Environmental, and Architectural Engineering, University of Colorado Boulder, UCB 428, ECOT 441, Boulder, CO 80309-0248; email: frederick.rankin@colorado.edu.

ABSTRACT

During in situ groundwater remediation, a chemical or biological amendment is introduced into the aquifer to react with and degrade the contaminated groundwater. Degradation reactions only occur where the amendment and contaminant molecules are sufficiently close that they can react. Thus, maximizing the degree to which the amendment can be spread throughout the contaminant plume is critical for effective in situ remediation. Spreading is driven by spatial variations in velocity, which reconfigure the contaminant and amendment plumes, elongate the interface between them, increase the contact area on which reaction can take place, and sharpen concentration gradients near the plume boundaries, bringing the reactants together to react. Spatially varying velocity induced by injecting or extracting wells (active spreading) or by natural heterogeneity (passive spreading). The spatial patterns of heterogeneity and the range of values of hydraulic conductivity affect the degree of passive spreading and therefore significantly affect the amount of degradation that can occur during in situ remediation. We use numerical simulations of solute transport to evaluate the combined effect of active and passive spreading on contaminant degradation in aquifers with zonal heterogeneity that is typical of fluvial depositional environments. We evaluate different ranges of heterogeneity values between zones, and we demonstrate how the local plume geometry and the local velocity field affect the overall solute degradation. These results have implications for effective design of in situ groundwater remediation in aquifers that have well-characterized spatial distributions of hydraulic conductivity.

INTRODUCTION

During in situ remediation of contaminated groundwater, a chemical or biological amendment is introduced into a contaminant plume to react with and degrade the contaminant. Degradation reactions can only occur where the contaminant and amendment molecules are sufficiently close that they can be brought together by molecular diffusion, allowing them to react. As the

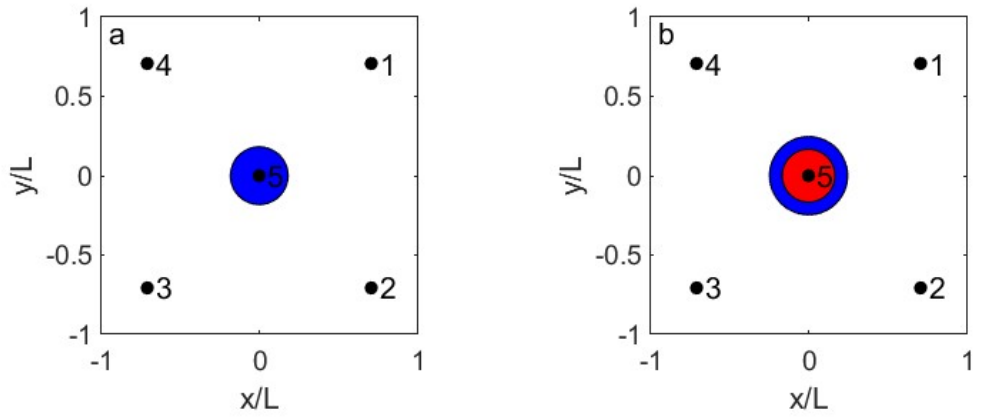

Figure 1. Portion of the model domain showing (a) position of contaminant plume prior to injection of the amendment and (b) positions of the contaminant plume (blue, species A) and amendment (red, species B) after injection of the amendment. Small black circles are wells. open circles are extraction wells. The distance between well 5 and any of the outer wells is *L*.

amendment is introduced into the contaminant plume (progression from Fig. 1a to Fig. 1b), the amendment (red plume in Fig. 1) flows radially outward from the injection well, forcing the contaminant (blue plume in Fig. 1) to also move radially outward. Although both the contaminant and amendment occupy a substantial volume of the aquifer, they are only in contact with each other along the interface between the plumes; thus, reaction can only occur along the area of the plume interface. The success of in situ remediation depends on the degree to which the amendment plume can be spread into the contaminant plume to increase the contact area between the two.

Spreading is the process by which a spatially or spatio-temporally varying velocity field reconfigures the plume geometry without changing the volume occupied by the plume. Spreading can elongate the plume interface leading to a larger contact area over which reactions can occur. As the plume interface is elongated, the concentration gradients along the interface can increase, increasing the diffusive mass flux that drives the molecules toward the plume interface, thereby increasing the rate of reaction. Spreading can be active or passive. With active spreading, spatially or spatio-temporally varying velocity fields are created by injecting or extracting water through wells in the aquifer. With passive spreading, spatially varying velocity occurs naturally due to aquifer heterogeneity, as groundwater flows preferentially toward high permeability materials and away from low permeability materials.

Several prior studies have evaluated the placement of wells and the injection and extraction schedule that best enhances degradation reactions during in situ remediation. Through numerical simulations, Sather et al. (2022) found that the overall amount of reaction is maximized when the plume interface is orthogonal to the local groundwater velocity. Thus, they recommend an active spreading sequence that first stretches the plume interface along one direction, and then drives flow in the direction orthogonal to the stretched interface. While heterogeneity (i.e., passive spreading) tends to enhance spreading (Neupauer et al., 2014), some active spreading protocols, defined by the locations of wells and their injection and extraction rates, in heterogeneous aquifers produce less reaction than the same scenarios in homogeneous aquifer (Quinn et al., 2022).

The goal of this work is to investigate how heterogeneity patterns affect spreading and reaction within an active spreading remediation system. Sather et al. (2022) evaluated spreading and reaction in heterogeneous aquifers in which heterogeneity was represented by smoothly varying random fields. They evaluated several active spreading protocols and found that the amount of reaction increases as heterogeneity increases for most active spreading protocols and heterogeneity patterns, except for the situations that causes the plume to constrict, which was dependent on the spatial pattern of heterogeneity. Quinn et al. (2022) evaluated patterns of zonal heterogeneity, with one zone of low or high hydraulic conductivity embedded in an otherwise homogeneous aquifer. They found that reaction is enhanced if active spreading can direct the plume interface into a zone of high hydraulic conductivity, but reaction is reduced (relative to a homogeneous aquifer) if the plume interface is directed into a zone of low hydraulic conductivity. In this work, we consider aquifer heterogeneity that follows a facies model. The results of the three different hydraulic conductivity models (smoothly varying random fields, Sather et al. 2022; discrete zones, Quinn et al. 2022; and facies model, this work) should provide an overarching conclusions about the role of patters of spatial heterogeneity on spreading and reaction with active spreading protocols during in situ remediation.

THEORY

We consider flow and reactive transport in a two-dimensional, square, confined, isotropic aquifer, with heterogeneous hydraulic conductivity. We neglect ambient groundwater flow, and we allow flow to be generated from injections and extractions at four fully penetrating wells. We assume that the aquifer initially contains a circular plume of species A (contaminant) with uniform concentration C_{Ao} surrounding a circular plume of species B (amendment) with uniform concentration C_{Bo}. A schematic of the aquifer, wells, and initial distributions of chemical species is shown in Figure 1a. We assume that species A and B reactive instantaneously and irreversibly following the model A + B → C.

The governing equation of reactive transport of species A, B, and C is given by

$$\frac{\partial C_i}{\partial t} = -\nabla \cdot \left(\mathbf{v} C_i \right) + \nabla \cdot \mathbf{D} \nabla C_i + R_i \tag{1}$$

where $C_i(x,y,t)$ is the concentration of species i (i = A, B, C) as a function of spatial position $\mathbf{x}$ = (x,y) and time t, $\mathbf{v}$ is groundwater velocity, R_i is the reaction rate of species i ($R_A = R_B = -R_C$), and $\mathbf{D}$ is the dispersion tensor given by

$$\mathbf{D} = \begin{bmatrix} D_{xx} & D_{xy} \\ D_{yx} & D_{yy} \end{bmatrix} \tag{2}$$

where

$$
\begin{aligned}
D_{xx} &= \alpha_L \frac{v_x^2}{|\mathbf{v}|} + \alpha_T \frac{v_y^2}{|\mathbf{v}|} \\
D_{yy} &= \alpha_T \frac{v_x^2}{|\mathbf{v}|} + \alpha_L \frac{v_y^2}{|\mathbf{v}|} \\
D_{xy} &= D_{yx} = (\alpha_L - \alpha_T) \frac{v_x v_y}{|\mathbf{v}|}
\end{aligned} \tag{3}
$$

where α_L and α_T are longitudinal and transverse dispersivity, respectively, and $\mathbf{v} = [v_x\ v_y]^T$ is the groundwater velocity vector, given by

$$
\mathbf{v} = -\frac{K}{n} \nabla h \tag{4}
$$

where K is hydraulic conductivity, n is porosity, and h is hydraulic head obtained by solving the groundwater flow equation, given by

$$
S_s \frac{\partial h}{\partial t} = \nabla \cdot (K \nabla h) + \sum_{j=1}^{N_w} Q_j(t)\, \delta(\mathbf{x} - \mathbf{x}_{wj}) \tag{5}
$$

where $h(x,y,t)$ is head as a function of spatial position (x,y) and time t, S_s is specific storage, Q_j is the injection rate per unit aquifer thickness in well j (j = 1, 2, … N_w), $\mathbf{x}_{wj}$ is the location of well j, N_w is the number of wells, and K is the spatially varying hydraulic conductivity. The hydraulic conductivity model is a facies model that assigns a material type to a grid based on the overall proportion of each material and the probability of transitioning from one material type to another.

The initial condition on (1) is shown in Figure 1b and the boundary conditions are $\nabla C_i \cdot \mathbf{n} = 0$ on all boundaries, where $\mathbf{n}$ is the outward unit normal vector. The initial condition for (5) is $h = h_o$ for all $\mathbf{x}$, and the boundary conditions are

$$
\begin{aligned}
&h = h_o \quad \text{at} \quad x = \pm L_x / 2 \\
&\frac{\partial h}{\partial y} = 0 \quad \text{at} \quad y = \pm L_y / 2
\end{aligned} \tag{6}
$$

where L_x and L_y are the length of each side of the square aquifer in the x and y-directions, respectively.

We used T-PROGS (Carle, 1999) to develop two different two-material distribution (Figure 2). The hydraulic conductivities of the materials were varied as shown in Table 1. We solved (5) using MODFLOW-2005 (Harbaugh et al. 2005), using a two-step active spreading protocol with the injection rates shown in Table 2. This is the same protocol that was used by Quinn et al. (2022). The protocol is designed to stretch the plumes in the northwest-southeast

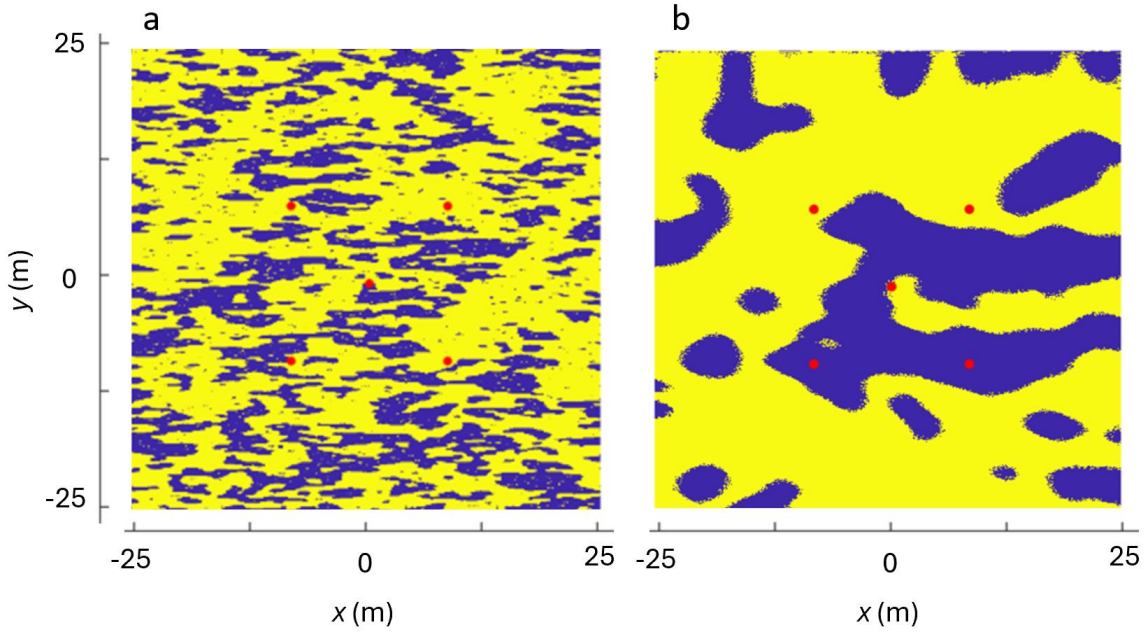

Figure 2. Material distributions using in the simulation. (a) Realization A. (b) Realization B. Material 1 is in blue and Material 2 is in yellow. Red dots show well locations.

Table 1. Hydraulic conductivity values for each material.

	Hydraulic Conductivity (m/d)		
Scenario	Material 1	Material 2	K_1/K_2
1	1	0.01	100
2	1	0.1	10
3	1	1	1
4	1	10	0.1
5	1	100	0.01

Table 2. Time-varying injection rates (negative rates indicate extraction).

			Injection Rate ($m^3/d/m$)			
Step	Start Time (d)	End Time (d)	Well 1, Q_1	Well 2, Q_2	Well 3, Q_3	Well 4, Q_4
1	0	30	-3.0	3.0	3.0	-3.0
2	30	60	0	3.0	-3.0	0

Table 3. Values of fixed parameters used in the simulations.

Parameter	Value
Specific storage, S_s	1 x 10^{-6} m
Porosity, n	0.31
Longitudinal dispersivity, α_L	0.20 m
Transverse dispersivity, α_T	0.020 m
Domain length, L_x and L_y	49.2 m
Coordinates of wells ($\mathbf{x}_{wj}$)	
Well 1	(-8.2 m, 8.2 m)
Well 2	(8.2 m, 8.2 m)
Well 3	(-8.2 m, -8.2 m)
Well 4	(8.2 m, -8.2 m)
Spatial discretization of finite difference grid	0.048 m x 0.048 m
Initial concentration of contaminant, C_{Ao}	1.0 mg/L/m
Initial concentration of amendment, C_{Bo}	2.0 mg/L/m

direction in Step 1, creating a plume interface that is aligned in the NW-SE direction almost everywhere, and then direct the flow in the southwest direction so that the flow direction is orthogonal to the plume interface, which is the condition that Sather et al. (2022) found to create the most degradation. We solve (1) using RW3D (Salamon et al. 2006), which uses random walk particle tracking. Instead of solving (1) directly, we simulate the transport of two conservative components, A+C and B+C, eliminating the reaction term in (1) (Gramling et al., 2002). Assuming a 1:1 mass ratio and 1:1 stoichiometric ratio of species A and B, the mass concentrations of species A, B, and C are obtained from the conservative components as

$$\begin{aligned} C_A(x,y,t) &= C_{A+C}(x,y,t) - C_C(x,y,t)/2 \\ C_B(x,y,t) &= C_{B+C}(x,y,t) - C_C(x,y,t)/2 \\ C_C(x,y,t) &= 2\min\left[C_{A+C}(x,y,t), C_{B+C}(x,y,t)\right] \end{aligned} \tag{7}$$

Other parameter values are shown in Table 3.

RESULTS

For each combination of the material distribution realizations in Figure 2 and the K_1/K_2 scenarios in Table 1, we calculated the degree of contaminant degradation at the midpoint and end of each step in Table 2. The degree of contaminant degradation is quantified as the relative mass of contaminant (species A) that has degraded by time t, denoted by $M_r(t)$, given by

$$M_r(t) = \frac{M_{Ao} - M_A(t)}{M_{Ao}} \tag{8}$$

where $M_A(t)$ is the mass of species A (contaminant) in the aquifer at time t, given by

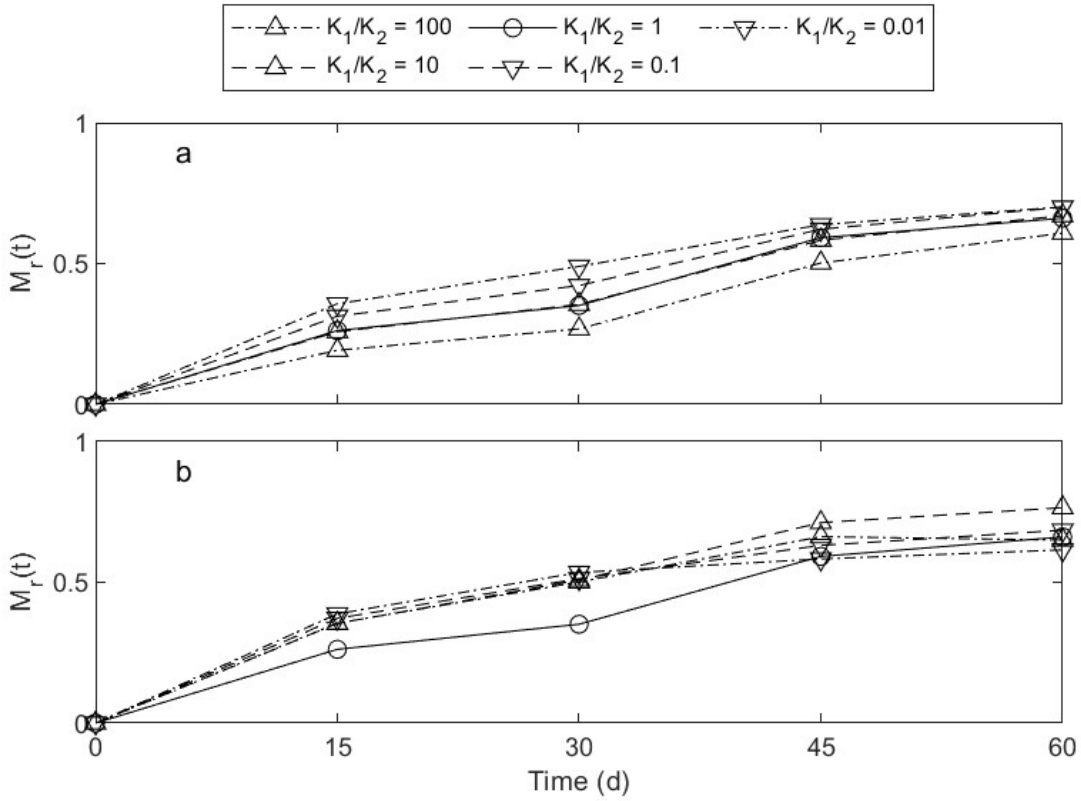

Figure 3. Degree of contaminant degradation for five values of K_1/K_2 for (a) material property realization A and (b) material property realization B.

$$M_A(t) = \iint_{x,y} nC_A(x,y,t)\,dx\,dy \tag{9}$$

and M_{Ao} is the initial mass of species A. Figure 3 shows plots of $M_r(t)$ vs. time for all five values of K_1/K_2 for both material property realizations. These results show that, for most cases, heterogeneity leads to more reaction compared to the homogeneous aquifer ($K_1/K_2 = 1$). For material property realization A, which has more frequent transitions from one material to the other, more reaction occurs when the hydraulic conductivity of material 1 (blue in Figure 2) is lower than the hydraulic conductivity of material 2 (yellow in Figure 2). For material property realization B, which has less frequent transitions from one material to the other, all heterogeneous aquifers have more reaction than the homogeneous aquifer, except for the case of $K_1/K_2 = 0.01$ at the final step. Note that this same value of K_1/K_2 had the most reaction for the other realization.

Figures 4 and 5 show the plumes of species A and B at four times during the active spreading protocol for $K_1/K_2 = 0.01$ for material property realizations A and B, respectively. In Figure 4, the plume interface is highly irregular and elongated, producing a high contact area

between the two species, resulting in high amount of reaction. In Figure 5, the plume interface is smooth, with a significant portion of species A (blue) trapped in the lower permeability material. Thus, species B tends to move away from species A, particularly at late times, leading to lower amounts of reaction compared to Figure 4.

CONCLUSION

In this work, we used numerical simulations to evaluate the influence of both active and passive spreading on contaminant degradation during in situ remediation. We modeled aquifer heterogeneity with a facies model, and we considered two material property distributions with two materials. Both distributions had the same proportion of the materials, but each distribution had a different transition probability from one material to the other. Material distribution realization A had more frequent transitions, while material distribution realization B had less frequent transitions. We evaluate the amount of reaction occurring in these aquifer for five different ratios of hydraulic conductivity of the two materials. The results show that the amount of degradation depends not only on the degree of heterogeneity, but also on the spatial pattern of heterogeneity and the position of the plumes within that spatial pattern.

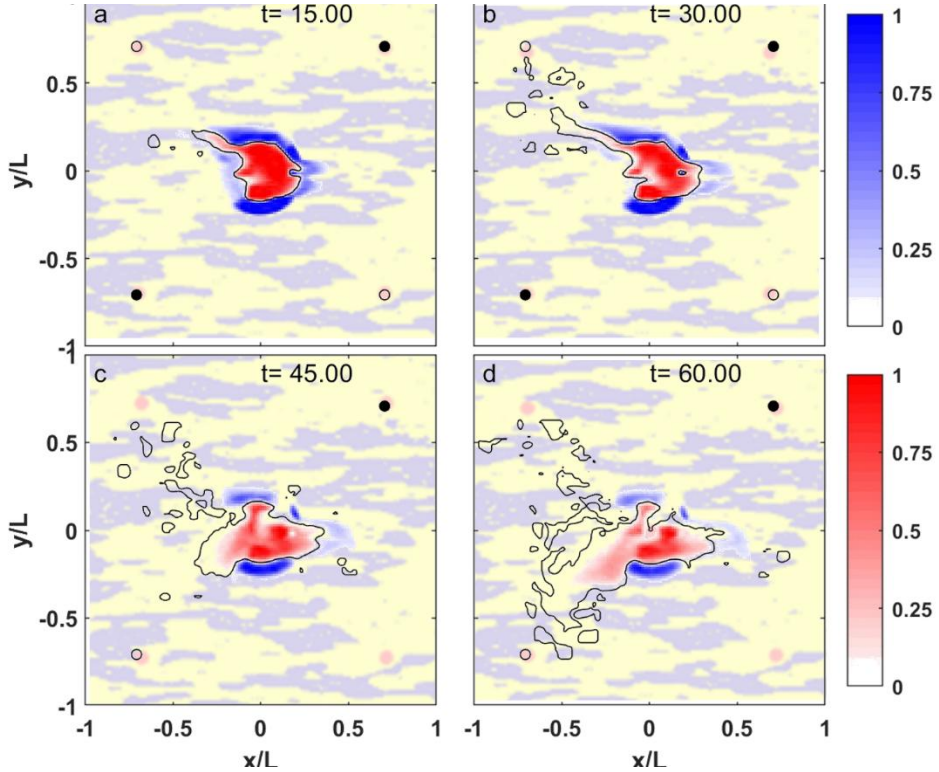

Figure 4. Normalized concentration distributions (normalized by initial concentration) of species A (blue, contaminant) and species B (red, amendment) at four times (in days) for the simulations with material property distribution A with $K_1/K_2 = 0.01$. The thin black line between the red and blue plumes is the plume interface. The small filled black circles are injection wells and small open circles are extraction wells. The background is the material distribution, with blue representing material 1 (K_1 = 1 m/d) and yellow representing material 2 (K_2 = 100 m/d).

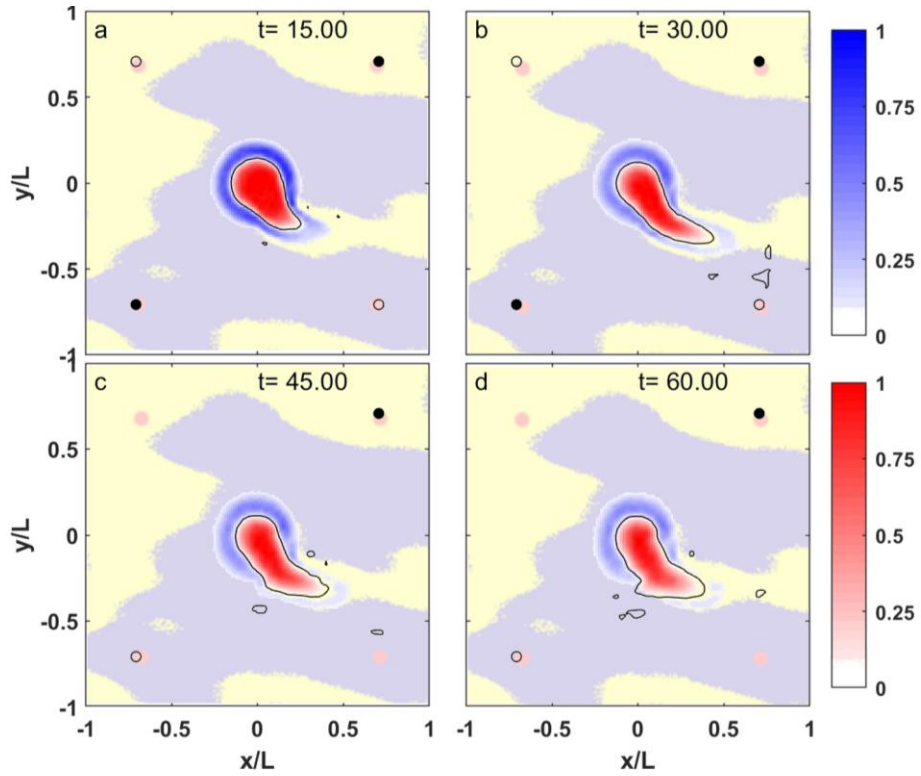

Figure 5. Normalized concentration distributions (normalized by initial concentration) of species A (blue, contaminant) and species B (red, amendment) at four times (in days) for the simulations with material property distribution B with $K_1/K_2 = 0.01$. The thin black line between the red and blue plumes is the plume interface. The small filled black circles are injection wells and small open circles are extraction wells. The background is the material distribution, with blue representing material 1 (K_1 = 1 m/d) and yellow representing material 2 (K_2 = 100 m/d).

REFERENCES

Carle, S.F. (2007). T-PROGS: Transition Probability Geostatistical Software Version 2.1, UCRL-SM-232880, Lawrence Livermore National Laboratory, Livermore, California.

Gramling, C.M., C.F. Harvey, and L.C. Meigs. (2002). Reactive transport in porous media: A comparison of model prediction with laboratory visualization. *Environmental Science & Technology*, 36(11), 2508-2514.

Harbaugh, A.W., (2005). MODFLOW-2005, the U.S. Geological Survey modular ground-water model -- the Ground-Water Flow Process: U.S. Geological Survey Techniques and Methods 6-A16.

Neupauer, R. M., J. D. Meiss, and D. C. Mays. (2014). Chaotic advection and reaction during engineered injection and extraction in heterogeneous porous media, *Water Resources Research*, 50, doi:10.1002/ 2013WR014057.

Quinn, J.T., R.M. Neupauer, L.J. Sather, D.C. Mays, J.P. Crimaldi, and E.J. Roth. (2022). Effects of active and passive spreading on mixing and reaction during in-situ groundwater

remediation, 2022 World Environmental and Water Resources Congress, American Society of Civil Engineers, Atlanta, Georgia, https://doi.org/10.1061/9780784484258.014.

Salamon, P., D. Fernández-García, and J.J. Gómez-Hernández. (2006). Modeling mass transfer processes using random walk particle tracking, *Water Resources Research*, 42, W11417.

Sather, L.J., R.M. Neupauer, D.C. Mays, J.P. Crimaldi, and E.J. Roth. (2022). Active spreading: Hydraulics for enhancing groundwater remediation, *Journal of Hydrologic Engineering*, 10.1061/(ASCE)HE.1943-5584.0002167.